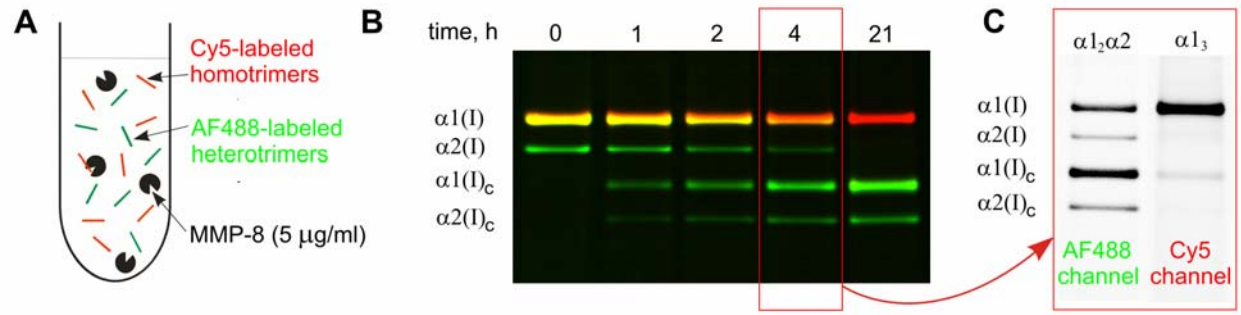

Figure S1. Collagen cleavage by interstitial MMPs in binary homo/heterotrimer mixtures

A, Schematic diagram of the experiment.

B, Gel electrophoresis of sample aliquots incubated with MMP-8 at 25 ^{o}C from 0 to 21 h. The composite image of the gel shows fluorescence of AF488-labeled heterotrimers in the green channel and fluorescence of Cy5-labeled homotrimers in the red channel. Yellow color indicates the presence of both hetero- and homotrimers.

C, Grayscale images of the AF488 and Cy5 fluorescence channels for the lane corresponding to 4 h incubation time, reproduced as MMP-8 panel of Fig. 1. Cleavage experiments with MMP-1, MMP-2, and MMP-13 were performed in a similar manner, except the concentration of each enzyme was adjusted to ensure optimal visualization of the cleavage kinetics (~50% of the heterotrimer cleavage after 2-8 h incubation time).

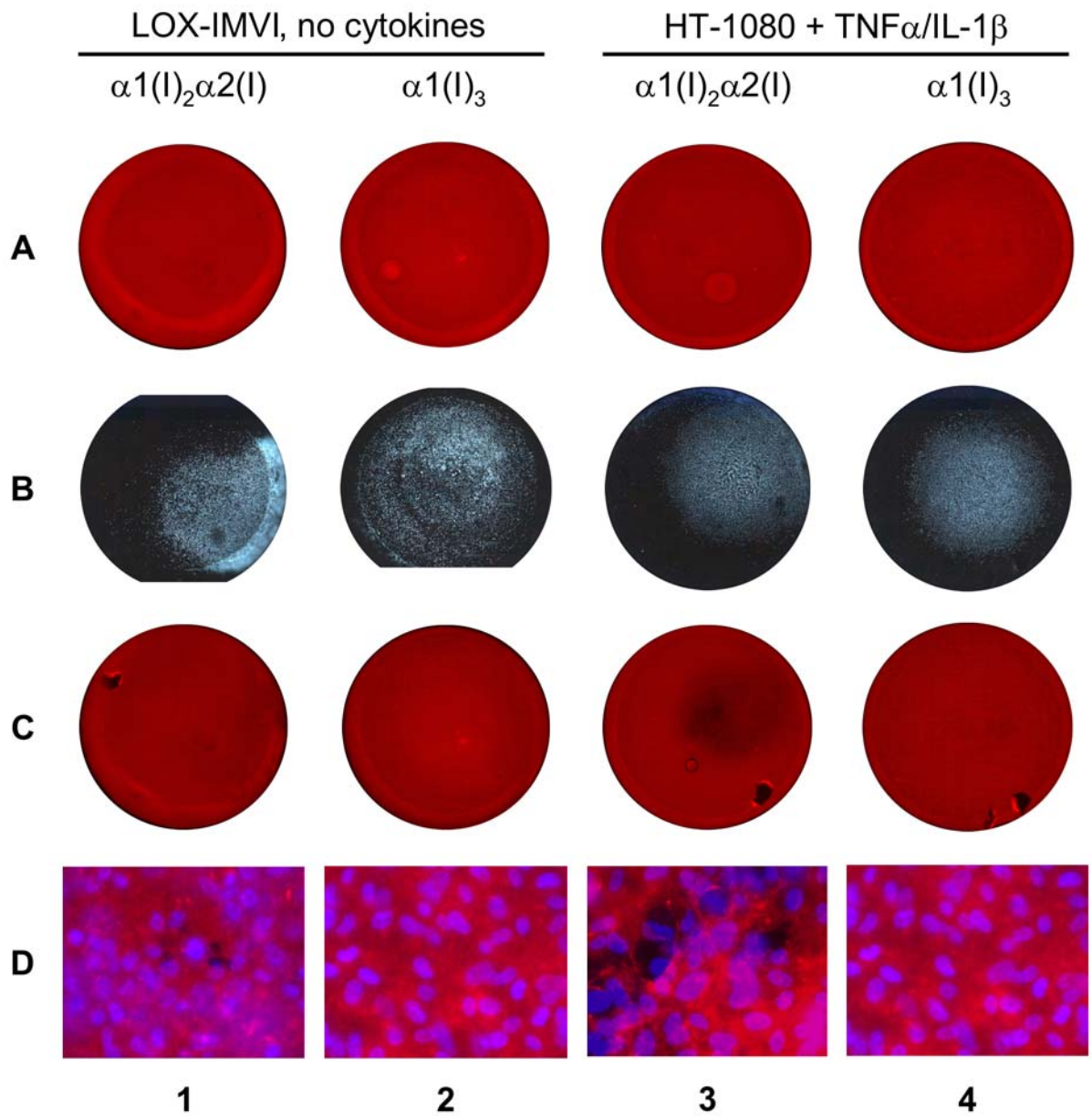

Figure S2. Pericellular degradation of collagen matrix by cancer cells after 4 day incubation at 37 °C with and without cytokine stimulation

A1-A4, Matrix before cell plating.

B1-B4, Cell nuclei after 4 day incubation.

C1-C4, Matrix after 4 day incubation.

D1-D4, Overlaid 40X wide-field fluorescence microscopy images of the matrix and cell nuclei.

The experiment was performed as described in Methods and Fig. 2 for mouse fibroblasts, except no cytokines were added to LOX-IMVI cells before or during the incubation. Only the matrix films reconstituted from type I heterotrimer fibers were degraded by either LOX-IMVI or HT-1080 cells. The heterotrimer matrix degradation by unstimulated LOX-IMVI cells was weaker, but small holes cut by the cells in the matrix were still clearly visible at 40X magnification (black areas in the middle of the D1 image). HT-1080 cells degraded most of the matrix underneath them (C3), and large holes were visible at 40X magnification (D3). No holes were observed in the homotrimer matrix.

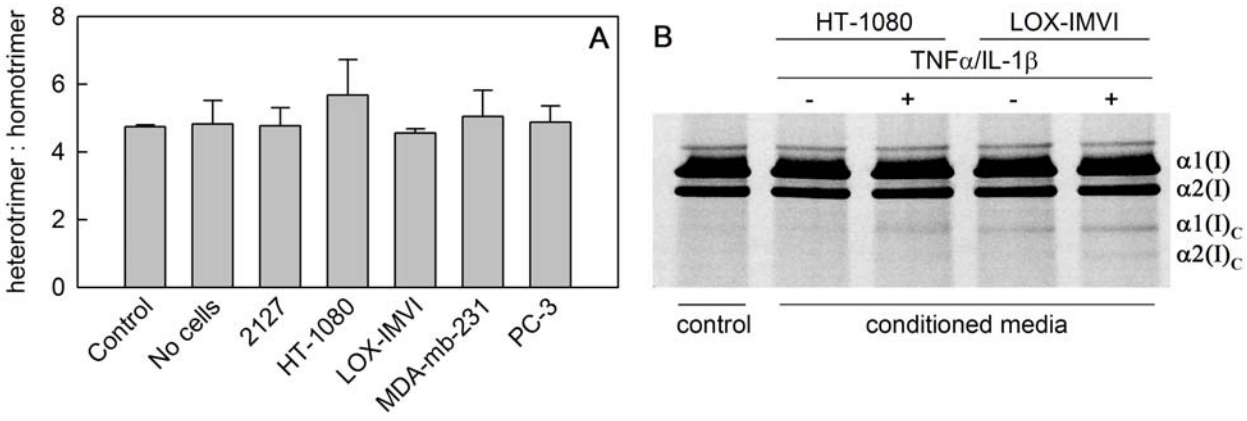

Figure S3. Collagenase activity in cell culture media

A, Cultured cancer cells were incubated at 37 ^{o}C for 24 h with freshly prepared media containing 5:1 mixture of heterotrimeric : homotrimeric human procollagen (2-5 μg/ml) prelabeled with AF488 and DyLight 549, respectively. The media was collected and heterotrimer : homotrimer ratio was re-analyzed by gel electrophoresis. The procollagen composition in the media was also checked in the freshly prepared, procollagen-supplemented media (control) and after incubating the media at 37 ^{o}C in a cell culture well without cells (no cells). Within the experimental error, no changes in the homotrimer : heterotrimer ratio were observed with any of the cells, indicating minimal (if any) procollagen cleavage by collagenases in the cell culture media during 24 h incubation.

B, Media conditioned by 24 h incubation with cancer cells in the presence of TNFα / IL-1β or without TNFα / IL-1β was treated with 1 mM p-aminophenylmercuric acetate (APMA) (to activate pro-MMPs), mixed 1:1 with fluorescently labeled collagen (0.1 mg/ml), incubated for 18 h at 25 ^{o}C, and analyzed by gel electrophoresis. No collagen cleavage was observed without the activation with APMA (data not shown). Only minimal collagen cleavage was observed after the activation with APMA, suggesting very low concentrations of mostly inactive soluble (pro)collagenases in the media after 24 h incubation with cells. At these concentrations, collagenases could not affect the ratio of type I collagen homotrimers and heterotrimers secreted by cells during 24 h incubation, confirming the results shown in panel A.

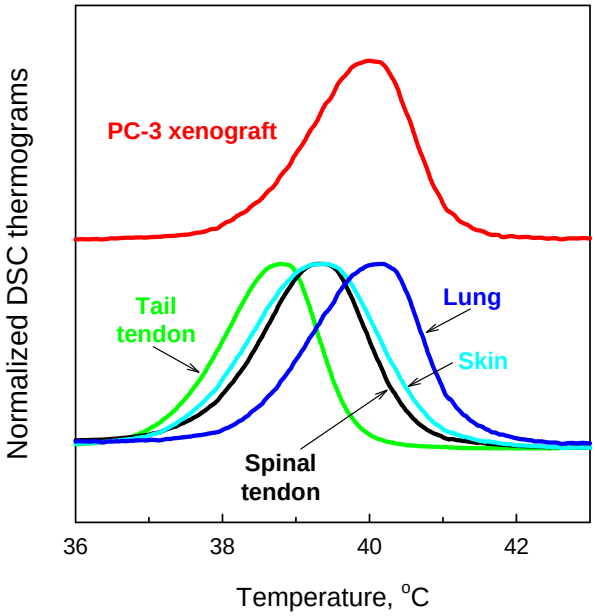

Figure S4. Comparison of total type I collagen extract from PC-3 xenograft tumor with type I collagen extracts from different mouse tissues

Tail-tendon, spinal-tendon, skin, and lung type I collagen were extracted from the same wild type animal. The variation in thermal stability of these molecules is caused by differences in posttranslational modification of type I collagen in these tissues. These differences are likely related to the normal functional temperature for each tissue, e.g., the normal temperature in tail tendons is expected to be substantially lower than in lung. Indeed, a significant increase in posttranslational modification and ~ 1 ^{o}C increase in the thermal stability of type I collagen is observed when the same skin fibroblasts are cultured at 40 ^{o}C instead of 37 ^{o}C (Cabral WA et al. Prolyl 3-hydroxylase 1 deficiency causes a recessive metabolic bone disorder resembling lethal/severe osteogenesis imperfecta. Nat Genet 2007;39:359-65).

DSC thermograms of total type I collagen extracted from PC-3 xenograft tumors were identical to heterotrimeric type I collagen from lungs of wild type mice, as might be expected due to elevated temperature inside growing tumors. However, because we were not able to extract sufficient amounts of homotrimeric type I collagen from lungs, DSC thermograms of heterotrimeric and homotrimeric spinal tendon collagens are shown in Fig. 4.

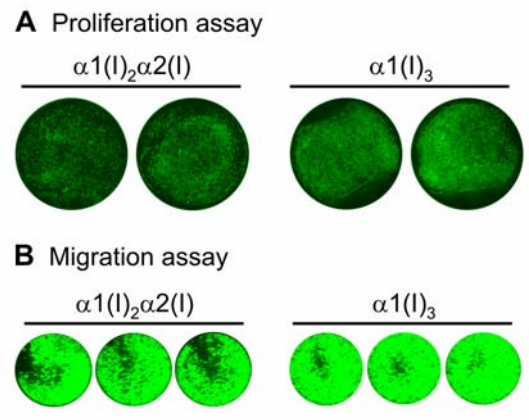

Figure S5. Proliferation and migration of cancer cells on matrix reconstituted from fibers of type I collagen hetero- and homotrimers

A, Fluorescence images of HT-1080 cells (green) after 4 day incubation on heterotrimeric and homotrimeric matrices and fluorescent labeling with calcein. Each circular area shows a cell culture well with the matrix deposited at the bottom of the well.

B, Fluorescence images of LOX-IMVI cell (green) migration. Each circular area shown in these images was blocked by plastic stoppers during cell plating and was clear of cells during initial incubation. Cell migration into this area was initiated by removal of the stoppers and allowed to proceed for 1 day before the cells were labeled with calcein and imaged.

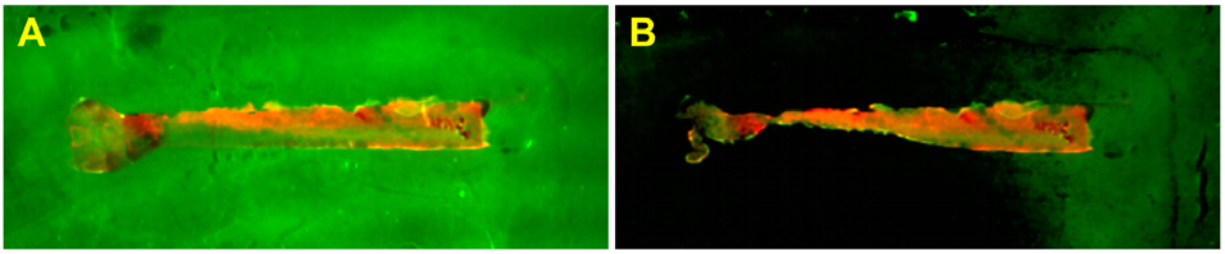

Figure S6. MMP-resistant homotrimer fiber roadways *in vitro*

A, Fluorescence image of a matrix strip (red) reconstituted from fibers of homotrimeric type I collagen on the surface of matrix (green) reconstituted from fibers of heterotrimeric type I collagen.

B, Fluorescence image of the same area after HT-1080 cells were plated in the left-hand-side and incubated for 5 days with 1 nM IL-1β and 10 nM TNF-α (1% FBS).

DyLight-649-labeled heterotrimeric matrix was deposited by *in vitro* fibrillogenesis as described in Methods for experiments shown in Figs. 2 and S2. The matrix was masked with a silicone spacer. Ice-cold solution of DyLight-549-labeled homotrimers in PBS was placed into a rectangular stripe cut out from the spacer followed by incubation at 32 ^{o}C (1 h) and 37 ^{o}C (overnight), to induce homotrimer fibrillogenesis. After removal of the silicone spacer, the resulting matrix was sterilized with 70% ethanol and washed. The matrix was imaged on the FLA5000 fluorescence scanner prior to cell plating and after 5 day incubation with cells. At the end of the incubation, the cells occupied the entire area.

Within the area initially occupied by the cells (left-hand-side), the heterotrimer matrix was almost completely degraded (black area in panel B) whereas the homotrimer matrix strip equally (or even more densely) populated with the cells remained largely intact. Note that heterotrimer fibers covered with homotrimers within the area of the homotrimer strip were also protected from the degradation, as indicated by green fluorescence from this area.

As discussed in the main text, collagen fibers play dual role in cancer invasion *in vivo*. They form a barrier for the invasion and they serve as tracks for cell migration. The present *in vitro* experiment confirms that the homotrimer tracks (here artificially deposited as a homotrimer strip) are resistant to degradation by cells (even when the degradation is stimulated with pro-inflammatory cytokines). The experiment shown in Fig. 4 suggests that such tracks might be formed only by cancer cells and not by cancer-associated fibroblasts. Thus, the MMP-resistant homotrimer and homotrimer-covered collagen fibers are likely to form along invasion tracks, promoting directed migration of cancer cells without forming a secondary invasion barrier (in contrast to MMP-susceptible heterotrimer fibers deposited by cancer associated fibroblasts throughout the entire tumor stroma).

Faster proliferation and migration of cells along homotrimer fibers (Fig. 5) may contribute to cancer invasion. However, we think that it is the resistance of these fibers to degradation by cancer-associated fibroblasts (the cells believed to be primarily responsible for formation and remodeling of tumor stroma) that may define homotrimer fibers as invasion roadways *in vivo*. This resistance gives cancer cells the ability to set up well-organized, MMP-protected collagen fibers within invasion tracks in otherwise disorganized tumor stroma.

On a cautionary note, panel B demonstrates only that roadways artificially constructed from homotrimer fibers are resistant to degradation by cancer cells. A true test for our hypothesis will require visualization of homotrimer fibers laid down by cancer cells in a complex tumor (or tumor-like) environment, which requires development of homotrimer-specific probes and is beyond the scope of the present work (see Discussion).